

## CH<sub>2</sub>OO Criegee biradical yields following photolysis of CH<sub>2</sub>I<sub>2</sub> in O<sub>2</sub><sup>†</sup>

Daniel Stone,<sup>a</sup> Mark Blitz,<sup>\*ab</sup> Laura Daubney,<sup>a</sup> Trevor Ingham<sup>ab</sup> and Paul Seakins<sup>ab</sup>

Cite this: *Phys. Chem. Chem. Phys.*, 2013, **15**, 19119

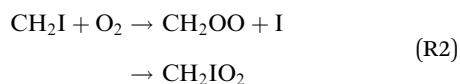
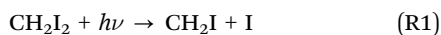
Received 13th June 2013,  
Accepted 6th September 2013

DOI: 10.1039/c3cp52466c

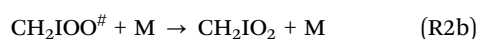
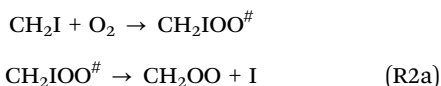
www.rsc.org/pccp

Yields of CH<sub>2</sub>OO and CH<sub>2</sub>IO<sub>2</sub> from the reaction of CH<sub>2</sub>I radicals with O<sub>2</sub> are reported as a function of total pressure, [N<sub>2</sub>] and [O<sub>2</sub>] at T = 295 K using three complementary methods. Results from the three methods are similar, with no observed additional dependence on [O<sub>2</sub>]. The CH<sub>2</sub>I + O<sub>2</sub> reaction has a yield of ~18% CH<sub>2</sub>OO at atmospheric pressure.

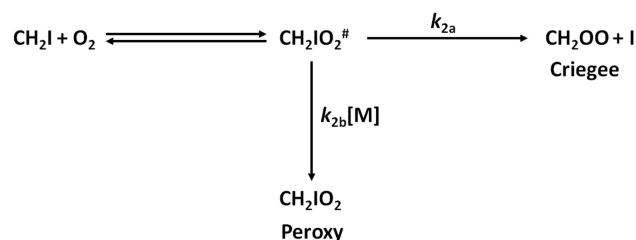
Criegee biradicals (CR<sub>2</sub>OO) are key reaction intermediates in the ozonolysis of unsaturated organic compounds,<sup>1</sup> and their involvement in the atmospheric oxidation of alkenes has long been postulated.<sup>2,3</sup> Despite much effort, direct observations of Criegee biradicals have only recently been reported for CH<sub>2</sub>OO<sup>4–8</sup> and CH<sub>3</sub>CHOO.<sup>9</sup> Photolysis of CH<sub>2</sub>I<sub>2</sub> in the presence of O<sub>2</sub> has been shown to produce CH<sub>2</sub>OO at low pressures through the reactions:<sup>5,10</sup>



However, the reaction between CH<sub>2</sub>I and O<sub>2</sub> proceeds *via* initial formation of an excited complex, CH<sub>2</sub>IOO<sup>#</sup>, which has the potential for collisional stabilisation to produce CH<sub>2</sub>IO<sub>2</sub> peroxy radicals (R2b) in competition with production of the CH<sub>2</sub>OO Criegee biradical (R2a) (Scheme 1):<sup>10</sup>



A number of investigations by Enami and co-workers<sup>11–13</sup> suggested production of HCHO and IO from CH<sub>2</sub>I + O<sub>2</sub>, but other studies,<sup>14,15,33</sup> including measurements in this laboratory,<sup>15</sup> have demonstrated that the production of IO results from



**Scheme 1** Chemical activation scheme to describe the reaction between CH<sub>2</sub>I and O<sub>2</sub> (R2), where the initially formed excited species CH<sub>2</sub>IO<sub>2</sub><sup>#</sup> either proceeds to produce CH<sub>2</sub>OO + I (*k*<sub>2a</sub>) or is collisionally stabilised to produce the CH<sub>2</sub>IO<sub>2</sub> peroxy radical or (*k*<sub>2b</sub>[M]).

secondary processes, and that IO is not a direct reaction product of (R2).<sup>14,15,33</sup>

The yields of CH<sub>2</sub>OO and CH<sub>2</sub>IO<sub>2</sub> from CH<sub>2</sub>I + O<sub>2</sub> were recently measured by Huang *et al.*<sup>10</sup> as a function of [N<sub>2</sub>], [O<sub>2</sub>] and [He] by monitoring the I atoms produced in (R1) and (R2a) *via* their infrared absorption owing to F'' = 4 → F' = 3 of the <sup>2</sup>P<sub>3/2</sub> → <sup>2</sup>P<sub>1/2</sub> spin-orbit transition at 7603.138 cm<sup>-1</sup>. Given the stoichiometry between CH<sub>2</sub>I and I in (R1), it is possible to infer the fraction of CH<sub>2</sub>I radicals producing CH<sub>2</sub>OO through comparison of the I atom yields from the instant photolytic production in (R1) and the slower production *via* (R2a). While there is potential for multi-photon dissociation of CH<sub>2</sub>I<sub>2</sub> to produce CH<sub>2</sub> + 2I, it is expected that this is relatively minor compared to production of CH<sub>2</sub>I + I.<sup>16–19</sup> Huang *et al.* showed that the yield of CH<sub>2</sub>OO decreases with total pressure, consistent with collisional stabilisation of the CH<sub>2</sub>IOO<sup>#</sup> intermediate to CH<sub>2</sub>IO<sub>2</sub>.

However, Huang *et al.* also reported significant differences in the I atom yields from (R2a) (and thus in CH<sub>2</sub>OO yields) between experiments performed in N<sub>2</sub> buffer gas and those performed in O<sub>2</sub>, indicating a much greater efficiency of O<sub>2</sub> for stabilisation of CH<sub>2</sub>IOO<sup>#</sup> to CH<sub>2</sub>IO<sub>2</sub> compared to N<sub>2</sub>, and an unusual interaction between CH<sub>2</sub>IOO<sup>#</sup> and O<sub>2</sub>.

In this work we report observations of the yields of CH<sub>2</sub>OO and CH<sub>2</sub>IO<sub>2</sub> from CH<sub>2</sub>I + O<sub>2</sub> following laser flash photolysis of CH<sub>2</sub>I<sub>2</sub>-N<sub>2</sub>-O<sub>2</sub> gas mixtures as a function of [N<sub>2</sub>], [O<sub>2</sub>] and total

<sup>a</sup> School of Chemistry, University of Leeds, UK. E-mail: m.blitz@leeds.ac.uk

<sup>b</sup> National Centre for Atmospheric Science, University of Leeds, UK

<sup>†</sup> Electronic supplementary information (ESI) available. See DOI: 10.1039/c3cp52466c



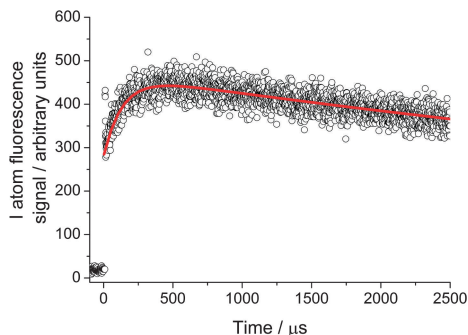


**Fig. 1** Iodine atom signal following photolysis of  $\text{CH}_2\text{I}_2$  in the presence of  $\text{O}_2$ . For this plot total pressure ( $N/V$ ) =  $3.27 \times 10^{17} \text{ cm}^{-3}$  ( $\sim 10$  Torr, predominantly  $\text{N}_2$ );  $[\text{O}_2] = 4.02 \times 10^{15} \text{ cm}^{-3}$ ;  $[\text{CH}_2\text{I}_2] = 5.03 \times 10^{12} \text{ cm}^{-3}$ . The time resolution is such that iodine production from photolysis and reaction can be identified. The fit to eqn (1) is shown by the solid line.

pressure using several complementary methods at total pressures between 25 and 450 Torr. Experiments were initially performed to monitor I atom fluorescence, thus enabling inference of the yields of  $\text{CH}_2\text{OO}$  and  $\text{CH}_2\text{IO}_2$  in the manner described by Huang *et al.*<sup>10</sup> Subsequent experiments monitored the yields of HCHO from reactions of  $\text{CH}_2\text{OO}-\text{CH}_2\text{IO}_2$  in the presence of excess  $\text{SO}_2$  or NO by laser-induced fluorescence (LIF) of HCHO at  $\lambda \sim 353.1$  nm. Full experimental details are given in the ESI.† All experiments were performed at  $T = 295$  K unless stated otherwise.

Fig. 1 shows the typical I atom signal following photolysis of  $\text{CH}_2\text{I}_2-\text{O}_2-\text{N}_2$ . The instantaneous photolytic production of iodine atoms through (R1) can be clearly distinguished from the subsequent growth in (R2a). The I atom signals were analysed using eqn (1):

$$[I]_t = S_0[\exp(-k_{\text{loss}}t)] + \frac{S_1k_2'}{k_2' - k_{\text{loss}}}[\exp(-k_{\text{loss}}t) - \exp(-k_2't)] \quad (1)$$

where  $[I]_t$  is the iodine atom signal at time  $t$ ,  $S_0$  is the amplitude of the instant photolytic signal resulting from (R1),  $S_1$  is the amplitude of the iodine atom signal resulting from the slower growth process occurring after photolysis,  $k_2'$  is the pseudo-first-order rate coefficient for (R2) (*i.e.*  $k_2' = k_2[\text{O}_2]$ ), and  $k_{\text{loss}}$  is the rate coefficient representing the slow loss of iodine atoms from the detection region *via* reaction or diffusion. A value of  $k_2 = (1.67 \pm 0.04) \times 10^{-12} \text{ cm}^3 \text{ s}^{-1}$  was determined in this work (see ESI†), in agreement with previous measurements of  $(1.40 \pm 0.35) \times 10^{-12} \text{ cm}^3 \text{ s}^{-1}$ ,<sup>20</sup> and  $(1.6 \pm 0.2) \times 10^{-12} \text{ cm}^3 \text{ s}^{-1}$ .<sup>21</sup> All errors quoted for this work are statistical at the  $1\sigma$  level unless stated otherwise.

The absolute iodine atom yield from reaction (R2a) is given by the ratio  $S_1/S_0$ , and was observed to decrease with increasing total pressure of  $\text{N}_2$ , consistent with production of the  $\text{CH}_2\text{OO}$  Criegee biradical at low pressures and stabilisation of the chemically activated  $\text{CH}_2\text{IO}_2^\#$  species to the  $\text{CH}_2\text{IO}_2$  peroxy radical at higher pressures. Solution of the I atom yield from (R2) ( $\Phi_1$ ), and thus the  $\text{CH}_2\text{OO}$  yield, is given by the Stern–Volmer relationship in eqn (2):

$$\frac{1}{\Phi_{1(\text{R}2)}} = 1 + \frac{k_{2b}}{k_{2a}}[M] \quad (2)$$

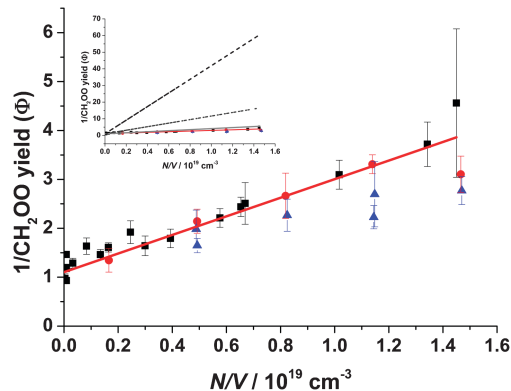
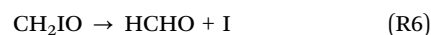
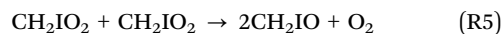
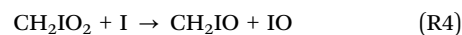
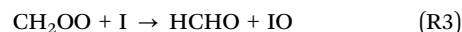


**Fig. 2** Stern–Volmer analyses for  $\text{CH}_2\text{OO}$  yields from  $\text{CH}_2\text{I} + \text{O}_2$  as a function of total pressure. Main panel shows results from this work monitoring iodine atom production (squares; intercept =  $1.08 \pm 0.12$ ; slope =  $(2.28 \pm 0.11) \times 10^{-19} \text{ cm}^3$ ), and HCHO production in the presence of  $\text{SO}_2$  (triangles; intercept =  $1.46 \pm 0.25$ ; slope =  $(0.95 \pm 0.24) \times 10^{-19} \text{ cm}^3$ ) and NO (circles; intercept =  $1.41 \pm 0.30$ ; slope =  $(1.33 \pm 0.31) \times 10^{-19} \text{ cm}^3$ ). Constraining the intercepts to unity for fits to  $\text{SO}_2$  and NO data gives slopes of  $(1.37 \pm 0.10) \times 10^{-19} \text{ cm}^3$  and  $(1.71 \pm 0.16) \times 10^{-19} \text{ cm}^3$ , respectively. Data shown for  $\text{SO}_2$  and NO were taken over a range of  $[\text{O}_2]$  ( $(0.1-7.8) \times 10^{18} \text{ cm}^{-3}$ ). A fit to all data reported in this work gives an intercept of  $1.10 \pm 0.23$  and a slope of  $(1.90 \pm 0.22) \times 10^{-19} \text{ cm}^3$  (shown by the solid line). Error bars shown on the plot and those given for the fits are  $1\sigma$ , with fits weighted to the experimental errors. Separate lines of best fit for results from the different methods are not shown for clarity but are given in the ESI.† The inset plot shows results from this work together with parameterisations given by Huang *et al.* for  $\text{N}_2$  (solid light grey line),  $\text{O}_2$  (broken black line) and air (broken dark grey line).

where  $\Phi_{1(\text{R}2)}$  is the iodine atom yield from (R2) (*i.e.*  $S_1/S_0$ ),  $k_{2b}/k_{2a}$  is the Stern–Volmer quenching coefficient, and  $[M]$  is the total number density of the system.

Fig. 2 shows the Stern–Volmer plot for reaction (R2). The intercept of the iodine atom Stern–Volmer plot is  $1.08 \pm 0.12$ , consistent with channel 2a being the dominant bimolecular process. The slope of the Stern–Volmer plot gives the Stern–Volmer quenching coefficient ( $k_{2b}/k_{2a}$ ), and is equal to  $(2.28 \pm 0.11) \times 10^{-19} \text{ cm}^3$  for these experiments, similar to the value of  $k_{2b}/k_{2a} = (3.1 \pm 0.2) \times 10^{-19} \text{ cm}^3$  reported by Huang *et al.*<sup>10</sup> for experiments in  $\text{N}_2$  buffer gas. For stabilisation of  $\text{CH}_2\text{IO}_2^\#$  by  $\text{O}_2$ , Huang *et al.* report a value of  $k_{2b}/k_{2a} = (4.09 \pm 0.32) \times 10^{-18} \text{ cm}^3$ . The iodine atom experiments in this work were conducted at low  $[\text{O}_2]$  ( $\sim 4 \times 10^{15} \text{ cm}^{-3}$ ) to ensure (R2a) was sufficiently slow to provide confidence in the resolution of the photolytic I atom production from the chemical I atom production. The effects of  $\text{CH}_2\text{IO}_2^\#$  stabilisation by  $\text{O}_2$  were thus investigated in the HCHO yield experiments.

Fig. 3a shows a typical kinetic trace for HCHO following photolysis of  $\text{CH}_2\text{I}_2-\text{O}_2-\text{N}_2$  in the absence of any additional co-reagent (*i.e.*  $\text{SO}_2$  or NO), in which HCHO is produced in the system by reactions (R3–R6):



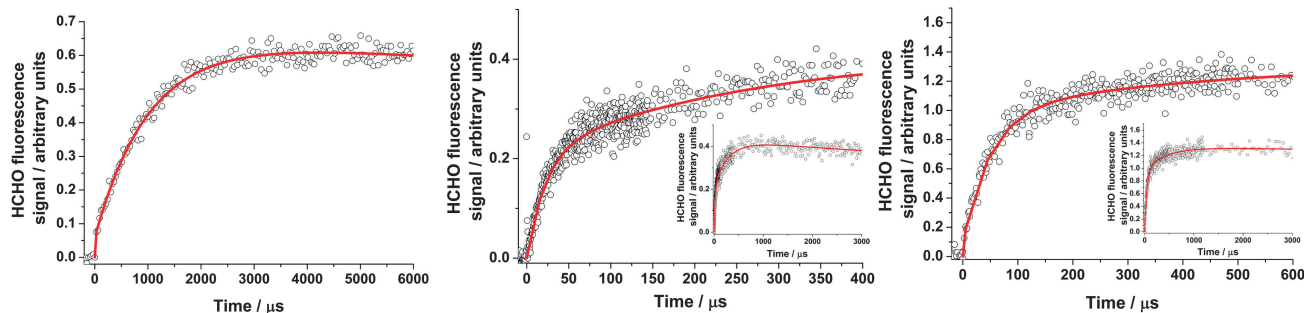


**Fig. 3** HCHO fluorescence signals following photolysis of  $\text{CH}_2\text{I}_2$  in the presence of  $\text{O}_2$ . Panel (a) shows HCHO signals at 150 Torr in the absence of any co-reagent with the fit to eqn (3). Panel (b) shows HCHO signals at 250 Torr in the presence of  $\text{SO}_2$ , with the fit to eqn (4). Panel (c) shows HCHO signals at 250 Torr in the presence of  $\text{NO}$ , with the fit to eqn (4). The inset plots in (b) and (c) show the evolution of the signals to longer times.

Although the HCHO production in this system is not strictly pseudo-first-order, Gravestock *et al.*<sup>15</sup> have shown that the growth from reactions (R3–R6) can be approximated to pseudo-first-order behaviour, and thus the data can be fitted using eqn (3).<sup>14,15</sup>

$$[\text{HCHO}]_t = S_0[\exp(-k_{\text{loss}}t)] + \frac{S_1 k_g'}{k_g' - k_{\text{loss}}} [\exp(-k_{\text{loss}}t) - \exp(-k_g' t)] \quad (3)$$

where  $[\text{HCHO}]_t$  is the HCHO signal at time  $t$ ,  $S_0$  is the amplitude of the HCHO signal at time zero,  $S_1$  is the maximum HCHO signal,  $k_g'$  is the pseudo-first-order rate coefficient for HCHO growth, and  $k_{\text{loss}}$  is the rate coefficient representing the slow loss of HCHO from the detection region *via* diffusion. Some initial HCHO production was observed owing to multi-photon photolysis of  $\text{CH}_2\text{I}_2$  and the subsequent rapid reaction of  $^3\text{CH}_2$  with  $\text{O}_2$ ,<sup>16–19</sup> with  $S_0$  typically no greater than 5–10% of  $S_1$ . In the present experiments  $k_g'$  was typically  $\sim 500 \text{ s}^{-1}$ , which is one to two orders of magnitude slower than the reactions occurring when  $\text{SO}_2$  or  $\text{NO}$  were added to the system. Simulations performed with the numerical integration package Kintecus<sup>22</sup> (provided in the ESI<sup>†</sup>) indicate that eqn (3) faithfully describes the yields of HCHO (*i.e.*  $S_1$ ) in this system. Reactions (R3–R6) imply that all the  $\text{CH}_2\text{OO}$  and  $\text{CH}_2\text{IO}_2$  react to form formaldehyde, *i.e.* all the  $\text{CH}_2\text{I}$  radicals are converted to HCHO. The recent study by Huang *et al.*<sup>10</sup> has demonstrated that the Criegee radical,  $\text{CH}_2\text{OO}$ , is formed with or near unity yields at low pressures from reaction (R2). The validity of 100% production of HCHO in the system can be tested at low pressures with Criegee reactions that produce formaldehyde. At low pressures the reaction between  $\text{CH}_2\text{OO}$  with  $\text{SO}_2$  is known to produce 100% HCHO,<sup>23</sup> and below we demonstrate that the total HCHO yield in the system is the same with and without the addition of  $\text{SO}_2$ , only the timescale for its formation varies.

Experiments conducted in excess  $\text{SO}_2$  or  $\text{NO}$  did not result in a decrease in the HCHO yield on addition of the co-reagent, indicating complete titration of both  $\text{CH}_2\text{OO}$  and  $\text{CH}_2\text{IO}_2$  to HCHO. In both cases biexponential growth of HCHO was observed,

as shown in Fig. 3b and c, with the observed HCHO signal in both cases described by eqn (4):

$$[\text{HCHO}]_t = S_0[\exp(-k_{\text{loss}}t)] + \frac{S_1 f k_{g1}'}{k_{g1}' - k_{\text{loss}}} [\exp(-k_{\text{loss}}t) - \exp(-k_{g1}' t)] + \frac{S_1 (1-f) k_{g2}'}{k_{g2}' - k_{\text{loss}}} [\exp(-k_{\text{loss}}t) - \exp(-k_{g2}' t)] \quad (4)$$

where  $[\text{HCHO}]_t$  is the HCHO signal at time  $t$ ,  $S_0$  is the amplitude of the HCHO signal at time zero,  $S_1$  is the maximum HCHO signal,  $k_{g1}'$  is the pseudo-first-order rate coefficient for the fast HCHO growth,  $k_{g2}'$  is the pseudo-first-order rate coefficient for the slower HCHO growth,  $f$  is the fractional contribution of the fast growth process to the total HCHO yield (and hence  $(1-f)$  is the fractional contribution of the slower growth process to the total HCHO yield), and  $k_{\text{loss}}$  is the rate coefficient representing the slow loss of HCHO from the detection region *via* diffusion.  $f$  is therefore related to the yield of the Criegee, eqn (2), as we demonstrate below. Again, in experiments conducted with a photolysis wavelength of 248 nm, some initial HCHO production was observed owing to multi-photon photolysis of  $\text{CH}_2\text{I}_2$  and the subsequent rapid reaction of  $^3\text{CH}_2$  with  $\text{O}_2$ ,<sup>16–19</sup> with  $S_0$  typically no greater than 5–10% of  $S_1$ . In experiments using a photolysis wavelength of 355 nm,  $S_0 = 0$ .

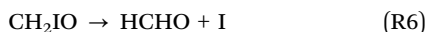
For both  $\text{SO}_2$  and  $\text{NO}$  experiments, the rate of the initial fast HCHO growth displayed a linear dependence on  $[\text{SO}_2]$  or  $[\text{NO}]$ , respectively, with  $k_{g1}'$  determined over the range 5000–60 000  $\text{s}^{-1}$ . The rate of the slower secondary growth was independent of  $[\text{SO}_2]$  or  $[\text{NO}]$ , and occurred at a similar rate to the HCHO growth observed in the absence of any additional co-reagent, and thus attributed to HCHO production *via* reaction (R3) or (R4–R6). The fact that  $k_{g1}' \gg k_{g2}'$  means that  $f$  is reliably determined, and that  $k_{g1}'$  is determined without any significant influence from the more complicated kinetics associated with the slower kinetics,  $k_{g2}'$ .

The fast HCHO in the presence of  $\text{SO}_2$  is consistent with production from  $\text{CH}_2\text{OO} + \text{SO}_2$ :



The slower growth of HCHO occurs as a result of reactions (R4–R6). Reaction of the peroxy radical with SO<sub>2</sub> is unlikely,<sup>24</sup> and the slower HCHO growth is not dependent on [SO<sub>2</sub>]. As [SO<sub>2</sub>] is in large excess over radicals in the system,  $k_{g1}'$  in eqn (4) is given by  $k_{g1}' = k_7[\text{SO}_2]$ , while  $k_{g2}'$  approximates the growth of HCHO through reactions (R4–R6). The returned value of  $f$  in this case is equal to the CH<sub>2</sub>OO yield.

Reactions of peroxy radicals with NO are typically fast (for example,  $k_{\text{CH}_3\text{O}_2+\text{NO}} = 7.7 \times 10^{-12} \text{ cm}^3 \text{ s}^{-1}$  at 298 K<sup>25</sup>), while Welz *et al.*<sup>5</sup> reported an upper limit for the rate coefficient for reaction of CH<sub>2</sub>OO with NO of  $< 6 \times 10^{-14} \text{ cm}^3 \text{ s}^{-1}$ . Therefore, we propose that the fast HCHO growth in experiments with NO results from the reaction of CH<sub>2</sub>IO<sub>2</sub> with NO (R8) followed by the rapid decomposition of CH<sub>2</sub>IO to HCHO and I in (R6),<sup>15</sup> with the slower growth resulting from (R3):



As [NO] is in large excess over the other radicals in the system,  $k_{g1}'$  in eqn (4) is therefore given by  $k_{g1}' = k_8[\text{NO}]$ , while  $k_{g2}'$  approximates the growth of HCHO through reaction (R3). The returned values  $f$  in this case are thus equal to the yields of CH<sub>2</sub>IO<sub>2</sub>.

While the slower growth of HCHO is not strictly pseudo-first-order, but is treated as such by eqn (4), simulations (described in the ESI<sup>†</sup>) show that the yields of HCHO from the two growth processes are well described by eqn (4) and the yields from the two processes (*i.e.*  $S_1$  and  $f$ ) are faithfully determined by fitting to eqn (4). In both systems, the rate of the fast growth process (6000–60 000 for SO<sub>2</sub>; 5000–20 000 s<sup>-1</sup> for NO) is significantly faster than that of the slower growth process ( $\sim 300$ –500 s<sup>-1</sup>), ensuring that the two growth processes are essentially decoupled and the HCHO yields from the two growth processes can be distinguished, and that the rate coefficient describing the fast growth is equal to that for the pseudo-first-order reactions, (R7) or (R8). We assign no kinetic information to  $k_{g2}'$  for either system, and as shown in the ESI<sup>†</sup> the approximation of the slower growth process to pseudo-first-order kinetics leads to uncertainties in the yields of only 2–3%.

As noted above, there was no change in the total HCHO yield in the system upon the addition of either SO<sub>2</sub> or NO, and this was observed to be the case at all total pressures. At low pressures where the CH<sub>2</sub>OO yield is close to unity, the addition of SO<sub>2</sub> leads to reaction (R7) and formation of HCHO with close to 100% yield.<sup>23</sup> In the ESI<sup>†</sup>, Fig. S3 compares the HCHO signal in the system with and without the addition of SO<sub>2</sub>. The fact that both traces observe the same amount of HCHO in the system adds validity to the assumption that in the absence of reagents, reactions (R3–R6), lead to 100% HCHO formation. At higher total pressures where CH<sub>2</sub>IO<sub>2</sub> formation is significant, the reason the HCHO yield is still 100% is because there is no reaction between the peroxy radical and SO<sub>2</sub>, which is in agreement with the literature,<sup>24</sup> and the peroxy radical is titrated to HCHO *via* (R4–R6). In the case of NO, it is the peroxy radical that reacts rapidly with the NO (R8) to form HCHO, but there is no significant reaction between the CH<sub>2</sub>OO and NO, in accord with the results from Welz *et al.*,<sup>5</sup> and therefore HCHO is formed on a slow timescale *via* reaction (R3). This again leads to 100% yield of HCHO in the system independent of total pressure, in accord with the data.

Thus, the fractional contributions of the fast and slow growth processes to the total HCHO yields in the presence of NO and SO<sub>2</sub> can be used to identify the yields of CH<sub>2</sub>OO and CH<sub>2</sub>IO<sub>2</sub> from the reaction of CH<sub>2</sub>I with O<sub>2</sub>. The fractional contribution of the fast growth process to the total HCHO yield in the presence of NO thus reflects the yield of CH<sub>2</sub>IO<sub>2</sub> from (R2) (*i.e.*  $Y_{\text{CH}_2\text{IO}_2} = k_{2b}[\text{M}]/(k_{2a} + k_{2b}[\text{M}]) = f_{\text{NO}}$  and  $Y_{\text{CH}_2\text{OO}} = k_{2a}/(k_{2a} + k_{2b}[\text{M}]) = 1 - f_{\text{NO}}$ ), while the fractional contribution of the fast growth process to the total HCHO yield in the presence of SO<sub>2</sub> reflects the yield of CH<sub>2</sub>OO from (R2) (*i.e.*  $Y_{\text{CH}_2\text{OO}} = k_{2a}/(k_{2a} + k_{2b}[\text{M}]) = f_{\text{SO}_2}$  and  $Y_{\text{CH}_2\text{IO}_2} = k_{2b}[\text{M}]/(k_{2a} + k_{2b}[\text{M}]) = 1 - f_{\text{SO}_2}$ ).

Fig. 2 also shows the Stern–Volmer analysis for CH<sub>2</sub>OO yields determined by the SO<sub>2</sub> and NO experiments (*i.e.* Stern–Volmer plots for  $1/f_{\text{SO}_2}$  and  $1/(1 - f_{\text{NO}})$ , respectively). Experiments with SO<sub>2</sub> (triangles) give  $k_{2b}/k_{2a} = (0.95 \pm 0.24) \times 10^{-19} \text{ cm}^3$ , while those with NO (circles) give  $k_{2b}/k_{2a} = (1.33 \pm 0.31) \times 10^{-19} \text{ cm}^3$ , with intercepts of  $1.46 \pm 0.25$  and  $1.41 \pm 0.30$ , respectively. Constraining the intercepts to unity in the fits to data from the SO<sub>2</sub> and NO experiments gives  $k_{2b}/k_{2a} = (1.37 \pm 0.10) \times 10^{-19} \text{ cm}^3$  and  $k_{2b}/k_{2a} = (1.71 \pm 0.16) \times 10^{-19} \text{ cm}^3$ , respectively.

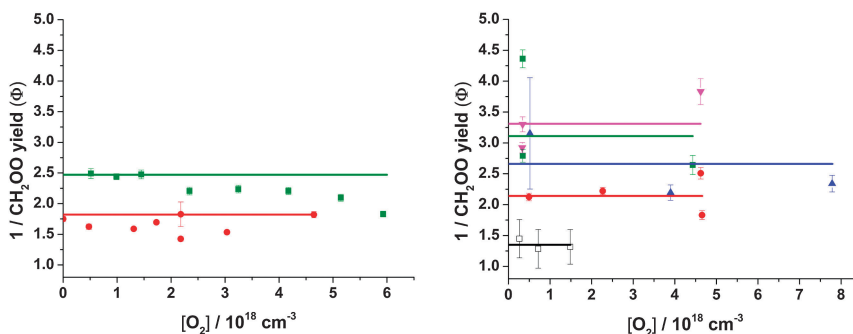


**Fig. 4** Inverse of CH<sub>2</sub>OO yields from CH<sub>2</sub>I + O<sub>2</sub> as a function of [O<sub>2</sub>] for experiments with (a) SO<sub>2</sub> at 150 Torr (circles) and 350 Torr (squares); (b) NO at 50 Torr (open squares), 150 Torr (circles), 250 Torr (triangles), 350 Torr (filled squares) and 450 Torr (inverted triangles). Horizontal lines show the average inverse CH<sub>2</sub>OO yield at each pressure for all experiments SO<sub>2</sub> (panel a) and NO (panel b). Error bars are 1σ in the fits to eqn (4).



Further details can be found in the ESI.† The relative errors in the SO<sub>2</sub> and NO experiments are typically larger than those for the iodine atom experiments owing to the need to fit a greater number of parameters in eqn (4) compared to eqn (1), and the smaller range of pressures in the Stern–Volmer plot for which the yields can be determined by the SO<sub>2</sub> or NO method (at low and high pressures, where one of CH<sub>2</sub>OO or CH<sub>2</sub>IO<sub>2</sub> dominates the HCHO growth it is difficult to resolve the two growth components, and thus to retrieve the relative yields, in the fit to eqn (4)). From Fig. 2, the fact that within error there is reasonable agreement in the CH<sub>2</sub>OO yields from the HCHO and the iodine atom experiments is further indication that all the sources of HCHO in each of the systems are understood and defined.

Experiments in both SO<sub>2</sub> and NO were performed over a range of O<sub>2</sub> concentrations, with measurements taken using 100% O<sub>2</sub> buffer gas in both cases (see Fig. 4), in order to test if O<sub>2</sub> has a significant effect on the CH<sub>2</sub>OO yield. In contrast to the work of Huang *et al.*,<sup>10</sup> no dependence of  $k_{2b}/k_{2a}$  on [O<sub>2</sub>] was observed in any of our measurements. A fit to all our data reported here gives  $k_{2b}/k_{2a} = (1.90 \pm 0.22) \times 10^{-19} \text{ cm}^{-3}$ , with an intercept of  $(1.10 \pm 0.23)$ . Huang *et al.* noted that their observed difference in CH<sub>2</sub>IO<sub>2</sub><sup>#</sup> stabilisation efficiency by N<sub>2</sub> and O<sub>2</sub> was an unusual result, with N<sub>2</sub> and O<sub>2</sub> often displaying similar collisional stabilisation efficiencies. It was proposed that O<sub>2</sub> may not be acting as a simple collision partner to remove excess energy in CH<sub>2</sub>IO<sub>2</sub><sup>#</sup>, but that there may be a reactive process occurring between O<sub>2</sub> and CH<sub>2</sub>IO<sub>2</sub><sup>#</sup>, potentially resulting in production of HCHO, IO and O<sub>2</sub>. However, an investigation of CH<sub>2</sub>I + O<sub>2</sub> by Gravestock *et al.*<sup>15</sup> could not identify IO as a product of the reaction even when more than 10% of O<sub>2</sub> was present at 30 Torr total pressure, and our measurements of HCHO yields in this work are not consistent with the production of HCHO from this reaction.

At present, there does not appear to be any simple explanation as to the differences between this work and the work of Huang *et al.* in the apparent yields of CH<sub>2</sub>OO and CH<sub>2</sub>IO<sub>2</sub> from CH<sub>2</sub>I + O<sub>2</sub> as a function of pressure. While the work of Huang *et al.* indicates a CH<sub>2</sub>OO yield of only ~4% in air at 760 Torr, our results indicate a yield of ~18%, with potentially significant implications for the oxidation chemistry of halogen containing organic compounds and for our understanding of atmospheric chemistry in marine regions with high concentrations of species such as CH<sub>2</sub>I<sub>2</sub>.<sup>26–32</sup>

In conclusion, we have measured the yields of CH<sub>2</sub>OO and CH<sub>2</sub>IO<sub>2</sub> from the reaction of CH<sub>2</sub>I radicals with O<sub>2</sub> as a function of total pressure and as a function of [N<sub>2</sub>] and [O<sub>2</sub>] using three complementary methods. Results from the three methods are similar, with no observed dependence of the CH<sub>2</sub>OO yield on [O<sub>2</sub>]. We estimate that the reaction between CH<sub>2</sub>I and O<sub>2</sub> reaction has a yield of ~18% of the CH<sub>2</sub>OO Criegee biradical at atmospheric pressure.

## Acknowledgements

The authors are grateful to the National Centre for Atmospheric Science (NCAS) and the Engineering and Physical Sciences Research Council (EPSRC, grant reference EP/J010871/1) for funding.

## References

- 1 D. Johnson and G. Marston, *Chem. Soc. Rev.*, 2008, **37**, 699–716.
- 2 R. Criegee and G. Wenner, *Justus Liebigs Ann. Chem.*, 1949, **564**, 9–15.
- 3 R. Criegee, *Angew. Chem., Int. Ed. Engl.*, 1975, **14**, 745–752.
- 4 C. A. Taatjes, G. Meloni, T. M. Selby, A. J. Trevitt, D. L. Osborn, C. J. Percival and D. E. Shallcross, *J. Am. Chem. Soc.*, 2008, **130**, 11883–11885.
- 5 O. Welz, J. D. Savee, D. L. Osborn, S. S. Vasu, C. J. Percival, D. E. Shallcross and C. A. Taatjes, *Science*, 2012, **335**, 204–207.
- 6 C. A. Taatjes, O. Welz, A. J. Eskola, J. D. Savee, D. L. Osborn, E. P. F. Lee, J. M. Dyke, D. W. K. Mok, D. E. Shallcross and C. J. Percival, *Phys. Chem. Chem. Phys.*, 2012, **14**, 10391–10400.
- 7 J. M. Beames, F. Liu, L. Lu and M. I. Lester, *J. Am. Chem. Soc.*, 2012, **134**, 20045–20048.
- 8 Y.-T. Su, Y.-H. Huang, H. A. Witek and Y.-P. Lee, *Science*, 2013, **340**, 174–176.
- 9 C. A. Taatjes, O. Welz, A. J. Eskola, J. D. Savee, A. M. Scheer, D. E. Shallcross, B. Rotavera, E. P. F. Lee, J. M. Dyke, D. K. W. Mok, D. L. Osborn and C. J. Percival, *Science*, 2013, **340**, 177–180.
- 10 H. Huang, A. J. Eskola and C. A. Taatjes, *J. Phys. Chem. Lett.*, 2012, **3**, 3399–3403.
- 11 S. Enami, T. Yamanaka, S. Hashimoto, M. Kawasaki, K. Tonokura and H. Tachikawa, *Chem. Phys. Lett.*, 2007, **445**, 152–156.
- 12 S. Enami, Y. Sakamoto, T. Yamanaka, S. Hashimoto, M. Kawasaki, K. Tonokura and H. Tachikawa, *Bull. Chem. Soc. Jpn.*, 2008, **81**, 1250–1257.
- 13 S. Enami, J. Ueda, M. Goto, Y. Nakano, S. Aloisio, S. Hashimoto and M. Kawasaki, *J. Phys. Chem. A*, 2004, **108**, 6347–6350.
- 14 J. Sehested, T. Ellermann and O. J. Nielsen, *Int. J. Chem. Kinet.*, 1994, **26**, 259–272.
- 15 T. J. Gravestock, M. A. Blitz, W. J. Bloss and D. E. Heard, *ChemPhysChem*, 2010, **11**, 3928–3941.
- 16 G. Hancock and V. Haverd, *Chem. Phys. Lett.*, 2003, **372**, 288–294.
- 17 H. M. Su, W. T. Mao and F. N. Kong, *Chem. Phys. Lett.*, 2000, **322**, 21–26.
- 18 U. Bley, F. Temps, H. G. Wagner and M. Wolf, *Ber. Bunsen-Ges. Phys. Chem.*, 1992, **96**, 1043–1048.
- 19 R. A. Alvarez and C. B. Moore, *J. Phys. Chem.*, 1994, **98**, 174–183.
- 20 A. J. Eskola, D. Wojcik-Pastuszka, E. Ratajczak and R. S. Timonen, *Phys. Chem. Chem. Phys.*, 2006, **8**, 1416–1424.
- 21 A. Masaki, S. Tsunashima and N. Washida, *J. Phys. Chem.*, 1995, **99**, 13126–13131.
- 22 J. C. Ianni, *Kintecus, Windows Version 2.80*, 2002, www.kintecus.com.
- 23 L. Vereecken, H. Harder and A. Novelli, *Phys. Chem. Chem. Phys.*, 2012, **14**, 14682–14695.



- 24 P. D. Lightfoot, R. A. Cox, J. N. Crowley, M. Destriau, G. D. Hayman, M. E. Jenkin, G. K. Moortgat and F. Zabel, *Atmos. Environ., Part A*, 1992, **26**, 1805–1961.
- 25 R. Atkinson, D. L. Baulch, R. A. Cox, J. N. Crowley, R. F. Hampson, R. G. Hynes, M. E. Jenkin, M. J. Rossi and J. Troe, *Atmos. Chem. Phys.*, 2006, **6**, 3625–4055.
- 26 C. M. Roehl, J. B. Burkholder, G. K. Moortgat, A. R. Ravishankara and P. J. Crutzen, *J. Geophys. Res., Atmos.*, 1997, **102**, 12819–12829.
- 27 L. J. Carpenter, W. T. Sturges, S. A. Penkett, P. S. Liss, B. Alicke, K. Hebestreit and U. Platt, *J. Geophys. Res., [Atmos.]*, 1999, **104**, 1679–1689.
- 28 L. J. Carpenter, *Chem. Rev.*, 2003, **103**, 4953–4962.
- 29 C. Ordonez, J. F. Lamarque, S. Tilmes, D. E. Kinnison, E. L. Atlas, D. R. Blake, G. S. Santos, G. Brasseur and A. Saiz-Lopez, *Atmos. Chem. Phys.*, 2012, **12**, 1423–1447.
- 30 A. Saiz-Lopez, J. M. C. Plane, A. R. Baker, L. J. Carpenter, R. von Glasow, J. C. G. Martin, G. McFiggans and R. W. Saunders, *Chem. Rev.*, 2012, **112**, 1773–1804.
- 31 A. Saiz-Lopez and R. von Glasow, *Chem. Soc. Rev.*, 2012, **41**, 6448–6472.
- 32 L. J. Carpenter, S. D. Archer and R. Beale, *Chem. Soc. Rev.*, 2012, **41**, 6473–6506.
- 33 T. J. Dillon, M. E. Tucceri, R. Sander and J. N. Crowley, *Phys. Chem. Chem. Phys.*, 2008, **10**, 1540–1554.

